PROGRESS OF INDIRECT DRIVE INERTIAL CONFINEMENT FUSION IN THE US

J. L. KLINE,[1] S. H. BATHA,[1] L. R. BENEDETTI,[2] D. BENNETT,[2] S. BHANDARKAR,[2] L. F. BERZAK HOPKINS,[2]
J. BIENER,[2] M. M. BIENER[2], R BIONTA,[2] E. BOND,[2] D. BRADLEY,[2] P. A. BRADELY,[1] T. BRAUN,[2]
D. A. CALLAHAN,[2] J. CAGGIANO,[2] T. CARDENAS,[1] C. CERJAN,[2] B. CAGADAS,[2] D. CLARK,[2] C. CASTRO,[2]
W. S. DAUGHTON,[1] E. L. DEWALD,[2] T. DÖPPNER,[2] L. DIVOL,[2] E. S. DODD,[1] R. DYLLA-SPEARS,[2] M. ECKART,[2]
D. EDGELL,[4] M. FARRELL,[3] J. FIELD,[2] F. FIERRO,[1] D. N. FITTINGHOFF,[2] M. GATU JOHNSON,[5] S. JOHNSON,[2]
G. GRIM,[2] N. GULER,[1] S. HAAN,[2] B. M. HAINES,[1] C. E. HAMILTON,[1] A. V. HAMZA,[2] E P. HARTOUNI,[2]
B. HAINES,[1] R. HATARIK,[2] K. HENDERSON,[1] H.W. HERRMANN,[1] D. HINKEL,[2] D. HO,[2] M. HOHENBERGER,[2]
D. HOOVER,[3] H. HUANG,[3] M. L. HOPPE,[3] O. A. HURRICANE,[2] N. IZUMI,[2] O. S. JONES,[2] S. KHAN,[2] B. J. KOZIOZIEMSKI,[2]
C. KONG,[2] J. KROLL,[2] G. A. KYRALA,[1] R. J. LEEPER,[1] S. LEPAPE,[2] E. LOOMIS,[1] T. MA,[2] A. J. MACKINNON,[2]
A. G. MACPHEE,[2] S. MACLAREN,[2] L. MASSE,[2] J. MCNANEY,[2] N. B. MEEZAN,[2] J. F. MERRILL,[1] E. C. MERRITT,[1]
J. L. MILOVICH,[2] D. S. MONTGOMERY,[1] J. MOODY,[2] A. NIKROO,[2] J. OERTEL,[1] R. E. OLSON,[1] A. PAK,[2]
S. PALANIYAPPAN,[1] P. PATEL,[2] B. M. PATTERSON,[1] T. S. PERRY,[1] R. R. PETERSON,[1] E. PICENO,[2] J. E. RALPH,[2]
R. B. RANDOLPH,[1] N. RICE,[3] H. F. ROBEY,[2] J. S. ROSS,[2] J. R. RYGG,[4] M. R. SACKS,[1] J. SAUPPE,[1] J. SALMONSON,[2]
D. SAYRE,[2] J. D. SATER,[2] J. SAUPPE,[1] M. SCHNEIDER,[2] M. SCHOFF,[3] D. W. SCHMIDT,[1] S, SEPKE,[2] R. SEUGLING,[2]
R. C. SHAH,[4] M STADERMANN,[2] W. STOEFFL,[2] D. J. STROZZI,[2] R. TIPTON,[2] C. THOMAS,[2] RPJ TOWN,[2] P. L. VOLEGOV,[1]
C.WALTERS,[2] M. WANG,[2] C. WILDE, [1] C. WILSON,[1] E WOERNER,[2] C. YEAMANS,[2] S. A. YI,[1] B. YOXALL,[2]
A. B. ZYLSTRA,[1] J. KILKENNY,[2] O. L. LANDEN, [2] W. HSING, [2] AND M. J. EDWARDS[2]

[1]Los Alamos National Laboratory, Los Alamos, NM, USA
[2]Lawrence Livermore National Laboratory, Livermore, CA, USA
[3]General Atomics, San Diego, CA, USA
[4]Laboratory for Laser Energetics, Rochester, NY, USA
[5]Massechusettes Institute of Technology, Boston, MA, USA

Abstract

Indirect drive converts high power laser into x rays using small high-Z cavities called hohlraums. X rays generated at the hohlraum walls drive a capsule filled with DT fusion fuel. Recent experiments have produced fusion yields exceeding 50 kJ where alpha heating provides ~3x increase in yield over PdV work. Improvements needed to approach ignition are challenging requiring optimization of the target/implosions and the laser to extract maximum energy. The US program has a three-pronged approach to maximize target performance each closing some portion of the gap. The first item is optimizing the hohlraum to couple more energy to the capsule while maintaining symmetry control. Novel hohlraum designs are being pursued that enable larger capsule to be driven symmetrically to both reduce 3D effects and increase energy coupled to the capsule. The second issue being addressed is capsule stability. Seeding of instabilities by the hardware used to mount the capsule and fill it with DT fuel remains a concern. Work such reducing the impact of the DT fill tubes and novel capsule mounts such as three sets of two single wire stands forming a cage, as opposed to the thin membranes currently used, are being pursed to reduce the effect of mix on the capsule implosions. There is also growing evidence native capsule seeds such as micro-structure may be playing a role on limiting capsule performance and dedicated experiments are being developed to better understand the phenomenon. The last area of emphasis is the laser. As technology progresses and understanding of laser damage/mitigation advances, increasing the laser energy seems possible. This would increase the amount of energy available to couple to the capsule and allow larger capsules potentially increasing the hot spot pressure and confinement time. The combination of each of these focus areas have the potential to produce conditions to initiate thermo-nuclear ignition.

1. INTRODUCTION

Indirect drive Inertial Confinement Fusion (ICF) converts high power laser light into x rays traditionally using small cylindrically-shaped, high-Z radiation cavities called hohlraums. A spherical capsule placed at the center of the hohlraum containing Deuterium-Tritium (DT) fuel absorbs x rays ablating the outer surface of the capsule and imploding via rocket motions. For “hot spot” ignition the primary approach to high gain ICF [1], the capsule has a layer of DT ice just inside the capsule with residual DT gas filling the central cavity. The capsules have traditionally been made of plastic (CH) or beryllium [2-6], but recently High Density Carbon (HDC) became the standard capsule material for experiments on the NIF. Compression of the DT gas forms a central "hot spot" where the fusion is initiated and through self-heating by capturing the alpha particles form the fusion reactions produces more energy than the PdV work needed to compress the gas. Once a robust burning plasma is formed in the "hot spot," ablation and heating of the inner surface of ice layer begins a propagating burn generating multi-Megajoule neutron yields.

Since the completion of the National Ignition Facility [7] and cryogenic target capabilities came online in 2010[8,9], much progress has been made towards ignition with more than a 20x increases in fusion neutron production and 3x increase in "hot spot" pressure, significant enhancements in diagnostic capabilities to understand capsule and hohlraum performance, advancement in laser facility optics damage mitigation techniques and precision. Early experiments using high-gain (defined as the ratio of the output neutron energy to the laser input energy) target-designs [10] highly optimized for peak performance, fell well below expectation. These experiments, which used silicon doped plastic (CH) capsules, under-performed due to the combination of 3D effects such as high mode 4-pi mix [11-15] and low mode asymmetries [16] amplified by high convergence [17,18]. Experiments following the initial high gain target designs traded the optimization for improved performance. The experiments, known as the "high foot" campaign [19] which also used silicon doped plastic capsules, increased the power in the initial portion of the laser pulse called the "foot." The increased power in the "foot" of the pulse has three primary effects: smoothing initial seeds for ablative hydrodynamic instability, increasing the scale-length of the ablation-front, and increasing the internal energy of the fuel reducing the theoretical compression and convergence. These experiments improved the performance by more than an order of magnitude and demonstrated self-heating of the "hot spot" for the first time in ICF [20-22]. However, the "high foot" implosions were ultimately limited in performance by laser backscatter reducing the amount of drive available for the targets and time-dependent cross-beam energy transfer affecting symmetry control [23-27], as well as feature driven shell perforations due to the tent [28-30]. Summaries of this work can be found in references by Meezan *et al*. [31] and Edwards *et al.* [17].

Over the past few years, target design changes have advanced implosion performance. Moving to low gas fill hohlraums have significantly reduced backscatter, increasing the drive available to the target as well as reducing laser damage concerns; have reduced by two orders of magnitude the production of suprathermal electrons inside the hohlraum, and have improved time-dependent symmetry control by reducing cross-beam transfer allowing implosion symmetry to be controlled directly through changes in the laser beam power balance. Moving to HDC capsules [32-35] enables higher velocity implosions with higher fuel internal energy that can still theoretically produce high gain. Top performing implosions now regularly exceed 50kJ of fusion output in a regime where the yield is dominated by self-heating via the alpha particles produced from the fusions reactions and "hot spot" pressures, ~300 Gbar, near ignition relevant conditions [36-38]. While the yield performance of indirect drive implosions on NIF have improved by more the 20x, there are still significant challenges to reaching ignition.

Moving forward, there will be a two pronged approach to increase performance of the current implosions. Improvements in the implosions quality by reducing remaining 3D effects such as low mode asymmetries and mix have the potential to increase performance rapidly for small improvements. The second approach is to increase the size of the capsule increasing the absorbed energy, while still controlling the implosion symmetry. Scaling to larger the target sizes improves the performance as $S^{4.5}$, where S is scale, but requires additional laser energy which scales as $\sim E_L * S^3$ where E_L is the laser energy unless implosion can be driven symmetrically without increasing the hohlraum size. This paper lays out the current understanding of the performance of indirect drive ICF implosions on the NIF and the approach to both improving performance as well as understanding what steps are needed to achieve ignition. The paper will be broken into broken improvement in the quality of the implosion in section II, both high and low mode asymmetries and scaling the current designs up in section III.

2. Implosion Quality

The most efficient means to reduce the required laser energy to achieve ignition is to generate "1D like" implosions. Such implosions can be driven to higher velocities and convergences leading to higher performance. Therefore, one of the key research focuses is reducing the sources of 3D imperfections [28]. The 3D effects are split into low mode asymmetries and high mode effects which can be further be categorized as feature driven perturbations, perforations, or mix due to capsule mounting hardware and fill tube or intrinsic 4-pi hydrodynamic instabilities such as Rayleigh-Taylor or Richtmyer-Meshkov that occur at interfaces.

2.1. Low mode asymmetries

As the Indirect Drive (ID) campaign moved to low gas fill hohlraum, control of implosion symmetry vastly improved with improved consistency between the simulations and measurements, i.e. no multipliers on the input laser power as with the gas filled hohlraum, as well as an empirical understanding making the designs more predictable. For indirect drive targets, control of implosion symmetry depends on the ability to deposit the laser energy in the hohlraum at the desired locations. The NIF laser is split into out cone beams compressed of beams at 44.5 and 50 with respect to the hohlraum axis and the inner cone beams at 23.5 and 30 with respect to the hohlraum axis. The outer cone beams are pointed at the hohlraum wall just inside the hohlraum near the laser entrance hole while the inner cone beams are pointed to the waist of the hohrlaum as in Figure 1. Symmetry control requires an understanding of the hohlraum dynamics that dictate the radiation pattern on the capsule. The dynamic nature of the hohlraum as the intense lasers ablate material of the hohrlaum wall leads to time dependent changes that affect where the laser beams deposit their energy [39]. The principle challenge is propagation of the inner cone laser beams to the waist of the hohrlaum. As shown in Figure 1a, expansion of the gold plasma ablated from the hohlraum by the laser pointed just inside the laser entrance holes, known as the "gold bubble," begins to block the path of the inner cone beams. Material ablated from the surface of the capsule also blows-off into the path of the inner cone beams. The work of Callahan *et al.* [40] shows an empirical relationship with implosion shape derived from experimental values related to the expansion rates of the plasma blow-off from the capsule and gold bubble, as well as the low density gas fill and energy in the picket of the laser pulse:

$$\sqrt{\frac{I_{picket}}{\rho_{fill}}\frac{\boldsymbol{t_{pulse}}}{R_{Hohl}}\frac{\boldsymbol{r_{cap}}}{R_{Hohl}}}$$

Where I_{picket} is the laser power in the picket, ρ_{fill} is the gas fill density, τ_{pulse} is the pulse length, R_{Hohl} is the hohlraum radius and r_{cap} is the capsule radius. The terms r_{cap}/R_{hohl} and τ/R_{hohl} address expansion of the capsule and wall respectively. There are two additional terms that set the symmetry control. Depending on the energy in the initial part of the laser known as the "picket" (Figure 1b) affects symmetry since the plasma expansion appears to depend on the energy. The hohlraum use a low pressure gas fill between 0.3 and 0.6 mg/cc. At these gas fills, backscatter appears negligible while leading to more symmetric implosions for fixed cone fraction [41]. These terms have a square root dependence. Using this formula, a linear relationship between the capsule shape is shown in Figure 1b as published in reference [40]. To develop this relationship, the formula in equation 1 is applied and the measured shape is adjusted to the shape corresponding to a 33% cone fraction, where the cone fraction is defined as the energy in the inner cone beams divided by the total laser energy. This adjustment normalizes the cone fraction for each experiment out of the comparison. This is enabled by the well behaved change in shape with laser cone fraction observed for the low gas filled hohlraums. Moreover, the trend is relatively independent of the capsule material which appears to be a higher order effect.

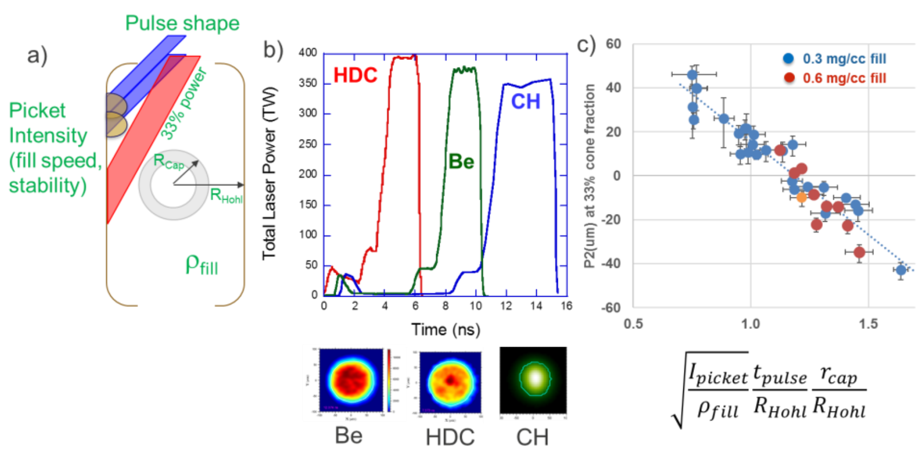

Figure 1: a) schematic of the hohlraum showing inner and outer cone beams with respect to the plasma expansion of the gold wall and capsule. B) Pulse shapes and x ray self emission for a HDC, a Beryllium, and a CH capsule. C) Plot of corrected symmetry vs empirical metric.

Controlling the capsule implosions symmetry is more than producing a nearly round implosion at peak compression. Preventing swings in the symmetry throughout the pulse is also important since energy in the swings reduces drive efficiency [42]. The low gas-filled hohlraum provides direct control of time-dependent implosion symmetry through adjusting the requested laser beam power balance rather than depending on time-dependent cross-beam energy transfer determined by evolving laser entrance hole plasma conditions. Data measured with principle diagnostics at different times through the laser pulse indicate the symmetry can be controlled without swings in shape as shown in figure 2 [43].

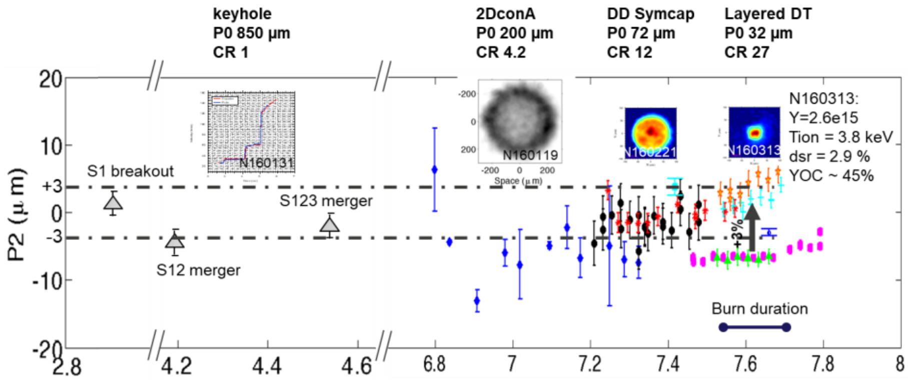

Figure 2: Data from VISAR early in time, backlight radiaography of the capsule during the imposion, x-ray self-emission from symcaps and layered DT implosions show the symmetry with the low gas-filled hohlraums remains nearly round.

While the shape of the x-ray self-emission and neutron pinhole measurements show the final hot spot shape can be controlled at the level believed to be needed for ignition, measurements suggest asymmetry in the compression of the cold fuel and potentially bulk motion of the capsule. These asymmetries may be comprised of a combination of both asymmetries arising from late time control due to beam propagation in the hohlraum or 3D effects due to the laser-target system which would require different solutions to improve the quality of the implosions. Figure 3 shows an example of the measurements using neutron activations diagnostics (NADs)[44] at various locations around the NIF target chamber. NADs measure the absolute number of neutrons above a given threshold through interacting of the neutrons with a high-Z activation foil. The neutron flux through the foil can be determined by counting the decay of the radioactive nuclei from the foil. Based on the measured flux from the NADS, the number of 14 MeV neutrons produced by an implosions can be measured in the direction of the foils. Reconstruction the flux from foils placed around the chamber is used as a measure of the fuel density since the flux is reduced by neutron collision in the dense fuel depending on the ρR, where ρ is density and R is the thickness of the fuel in a given direction. The reconstruction shown in Figure 3 for shot 171029-002, shows a common variation in the fuel thickness with higher flux, or thinner ice, is represented by red and lower flux, or thicker ice is represented by blue. The neutron flux variations is attributed to variations in the ρR (density x thickness) in the ice layer. Further analysis based on the timing of the signals on the neutron time of flight detectors (NTOFs) [45,46] detector show that there is also bulk motion of the capsule[47]. Before these asymmetries can be mitigated, their respective sources must be understood and diagnosed, which remains an important component of current programmatic efforts. Efforts to reconstruct the ice layer density using three orthogonal neutron images are being developed. The neutron imaging systems[48] can measure both the neutron measure both the neutrons generated by fusion reactions in the hot spot called the primary neutrons, as well as the neutron scattered by the cold compressed fuel called the downscattered neutrons. Since the downscattered neurons lose energy, an image gating system is used to discern the two populations of neutron. Using the both the primary and downscattered neutron images from three lines of site the shape of the cold fuel can be reconstructed [49]. In addition, a Compton scattering diagnostic that uses a high energy x ray backlighter and measure the Compton scattered photons is under development. This instrument will image the compressed cold fuel [50].

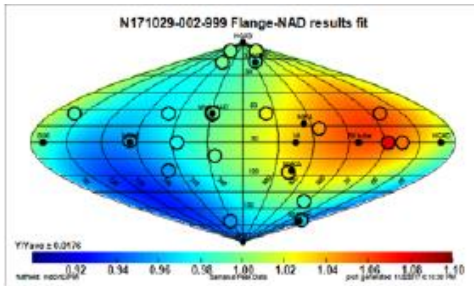

Figure 3: Map of the neutron yield variations as measured by the neutron flux measured by the NADS plance at different locations around the target chamber denoted by the circles for shot N171029 a HDC DT layered implosion.

In addition to improved diagnostics, an expert team has been examining other potential sources of asymmetries. For instance, just prior to the laser being fires, a set of shrouds used to block IR radiation form the chamber needed to control the target temperature near the DT triple point open. Vibrations due to the shroud opening are expected to damp-out prior to the shot. However, there are some indications this may not be true causing the target to move from its originally aligned position. Other potential issues are also being examined such as small laser peak power imbalances, power balance during the foot of the laser pulse, and diagnostic holes in the target. While these effects may produce small improvements of the current symmetry, they may account for an estimated ~1.5x improvement in performance [51].

The basic understanding in low gas filled hohlraum has led to improved performance. To capitalize on the knowledge to make the next advance in performance, modifications to the hohlraum design are in progress to improve late-time symmetry control, one of the limiting factors believed to further improvement in symmetry control. Figure 4 shows the leading candidates including foam liners [52,53] [Other references Moore??], rugby hohlraums [54-57], and the I-raum [58]. The foam lined hohlraums use pressure from the heated foam material to slow the wall expansion. The alternate hohlraum shape/geometry concepts delay enable the lasers to propagate to the designed location for longer laser pulses needed to move to larger capsules while controlling symmetry.

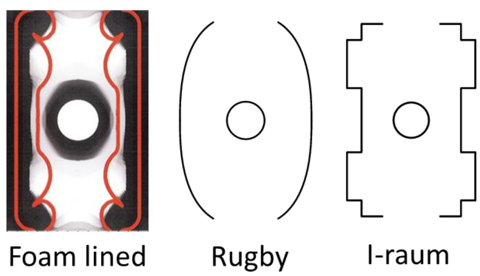

Figure 4: Three hohlraum designs being pursued to enable symmetry control for longer laser pulses.

2.2. High mode asymmetries

Mixing at the ablator/ice interface or ice/gas interface are responsible for the toughest challenges to removing the 3D nature of the implosions. It has long been know that mixing of the ablator and ice into the hot spot occurs as a result of surface roughness and engineering features such as the fill tube and tent used to mount the capsule in the hohlraum [29,30]. The strategy to mitigate the effect of the 3D engineering features for indirectly driving implosions is to reduce the perturbation seed [59,60]. For instance, the original fill tubes were 10 um in diameter. Recently, the size has been reduced to 5 um which has had a notable effect on performance. As shown in Figure 5, measurements using the hydro-growth radiography platform (HGR)[61] which using backlight radiography to measure the growth of perturbation show a notable reduce in growth due to the fill tube [52,53]. This is confirmed by x ray self-emission observations as well [62,63]. Using the 5 um fill tube on a DT layered implosions showed ~40% improvement in performance, and development of a 2 um fill tube is in progress. Similarly, there are several concepts to mitigate the capsule mounting hardware [64]. Tents designed to cover a smaller region near the capsule poles [65], small wire supports, or low density materials to separate mounting hardware from capsule.

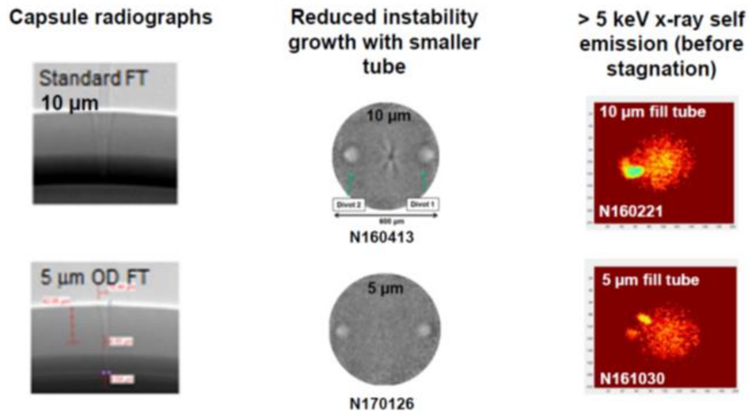

Figure 5 Experimental data from experiments comping 10 and 5 um file tubes showing a) capsule radiographs prior to shots, b) hydrogrowth radiography data from shots N160413 (10 um) and N170126 (5 um) using HDC capsules, and c) x ray self-emission measured from HDC DT layered experiments N160221 (10 um) and N161030 (5 um) [66].

In addition to the engineering features, other target characteristics such as surface roughness, internal ablator structure, and dopants are sources of hydrodynamic instabilities which degrade performance through mixing the shell or DT ice into the hot spot quenching the burn. The introduction of HDC [67,68] ablators have reduced ablative hydrodynamic instabilities both by improve surface finish which seeds the instability as well as ablative stabilization [69] due to the ablation rate and scale length of the ablation front. This has enabled higher velocity implosions that have a strong dependence on performance by enabling a larger ratio of the initial to final fuel mass, $v \sim ln(m_f/m_i)$ where v is velocity m_f is the final ablator mass and m_i is the initial ablator mass. That being said, the high convergences of the capsule implosions do make the performance sensitive to seeds for mix since the effects are amplified by compression [62]. Moreover, direct measurement of the instability growth in spherical geometry at high convergence is very challenging. Understanding 4-pi mix driven by hydrodynamic instabilities that occur at each interface and cover 4-pi steradians of the interface is challenging. 4-pi mix is typically understood through simulations and inferred through performance measured in experiments. For instance, mixing at the ablator/ice interface has a strong dependence on the dopant buried a few microns insider the inner surface of the capsule to improve stability through the Atwood number and to prevent Au m-band emission from the hohlraum from pre-heating the interface and mixing the ablator into the ice via the pressure difference across the boundary. This is illustrated in Figure 6 by both by simulations which show a more stable interface with the dopant which corresponds to an increase in performance [66,70]. High Resolution Velocimetry measurements of the expansion of the rear surface of ablator materials has shown that perturbations may be seeded by the microstructure in crystalline materials such as beryllium and diamond [reference?]. Efforts are underway to develop techniques that can measure mix at high convergence ratios (~10-20) related to the ablator/ice interfaces using x ray self-emission backlighting [71,72], high resolution imaging with a spherical crystal imager [73], and cylindrical implosion platforms [74].

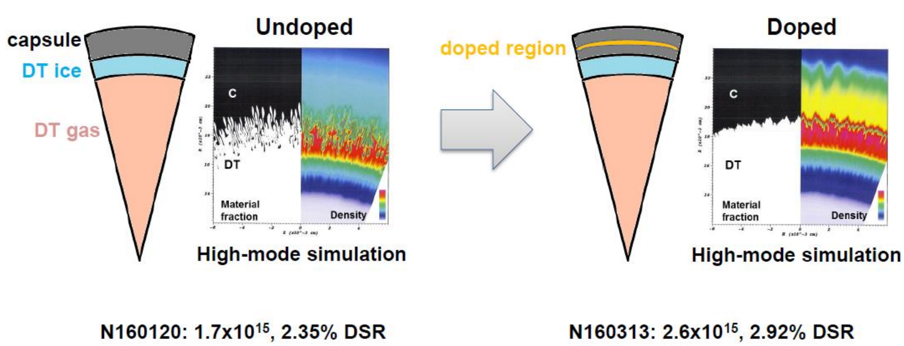

Figure 6: Data and simulations for a comparison of variation in tungsten dopant for HDC DT layered experiments showing imporve peformance with dopant and simulations that show the dopant stabilizes inteface [75].

3. Scaling to Larger Targets

Once implosion quality is maximized, the primary means to improve target performance is increasing the size of the capsule, i.e. scaling. Hydrodynamic scaling of the capsule size, scaling with sound speed transit times, preserves the implosion dynamics [76]. The yield without alpha heating, i.e. no burn, scale as $Y \sim S^{4.5}$, where Y is neutron yield and S is scale, due to the increase in the volume of the burn region and the additional confinement time due to the sound speed crossing time of the disassembly of the implosion. Combining the no alpha heating scaling with a model for alpha capture and using the hydro-scaling for the laser energy, $E \sim S^3$, and power, $P \sim S^2$, a curve based on the performance of an experiment can be derived as shown in Figure 7 [Reference]. The laser energy axis provides an estimate of the laser energy needed for the current quality implosions to reach a given yield. At laser energies near 3 Megajoules, implosions can reach igniting plasmas in which the alpha heating exceed all loss mechanisms. At laser energies in the range of 3.5-4 Megajoules, gains greater than one may be achieved. These estimates are based on the current quality of HDC implosions on NIF represented by the data points in pink. These estimates are based on the caveats that items that do not scale hydrodynamically such as laser spot sizes, laser plasma instabilities, heat conduction, 4-pi instability seeds, engineering feature driven mixing, alpha heating, and radiation hydrodynamics do not change rapidly when the target is scaled by small amounts, ~20-50%. These items can become less important with increased size or perhaps worse. Work is ongoing to evaluate how these physics elements affect the implosions as the target size increases. The real challenge to the scaling is estimating the level of confidence which becomes more uncertain as the estimates move away from the region where data is available. This is shown by the black dashed lines in Figure 7 which are notional at this time.

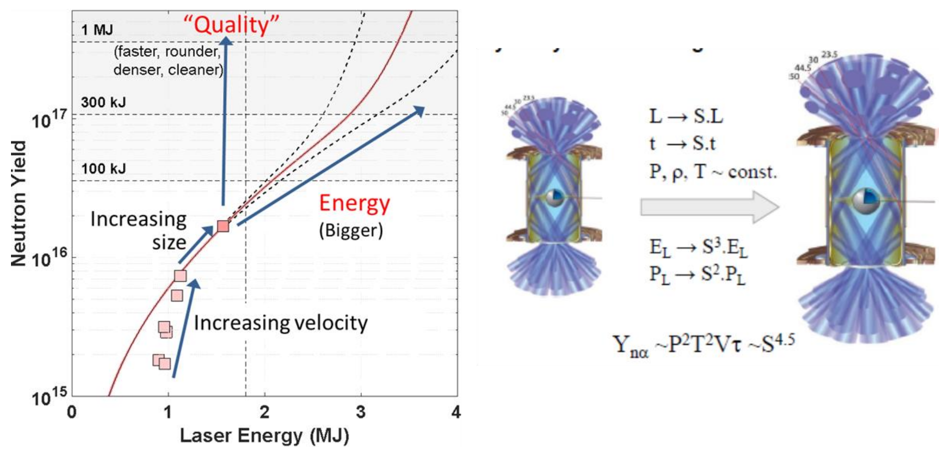

Figure 7: a) Estimated neutron yield based on no burn scaling from HDC data in pink with estimates for alpha self-heating. Black dashed curves represent notional bounds. B) Target scaling for the no burn case [references].

A significant effort to interpret and utilize the data to quantify the uncertainties for the scaling is underway. Uncertainty quantification beyond regions where data is available is a field of study unto itself. The work along with utilizing state of the art tools such as machine learning is being applied to this problem for ICF. Large ensembles of simulations with machine learning techniques are being used to determine the principle metrics for ICF implosion performance [77-80]. These metrics can then be calibrated with experimental data to form a baseline description.

Concurrently, with the experimental efforts to improve ICF performance, work is ongoing to improve laser performance generating higher laser energy and power. As technology progresses and understanding of laser damage/mitigation advances [81], possible paths to increasing the laser energy at 351 nm are being investigated, and there is always an option to move the 527 nm laser light has the potential to reach 5 MJ [82-84]. Increased laser energy enables capsules scaled-up in size to be driven as a means to improve performance with the caveat that laser plasma instabilities specifically Stimulated Brillouin Scattering at late times is still an unknown risk.

4. Conclusions

While considerable progress has been made toward thermonuclear ICF ignition over the past eight years, many challenges remain. The strategy going forward is to address phenomena that affect implosions quality, namely 3D effects due to both low and high mode asymmetries. Efforts will continue to reduce the remaining low mode asymmetries while making an asserted effort to address high mode mix. This entails reducing the effect of engineering features and addressing other sources of mix. Due to the difficulty in measuring mix for high convergence system and ongoing research into the understanding of mix, this effort will be a focus for the near future. Once the 1D nature of the implosion is maximized, the effort will turn to increasing scaling the capsule up and increasing implosion velocity. This will require improved drivers to maintain symmetry control with bigger capsules. All of these efforts will feed into design that can utilize higher laser energies to scale up the capsules.

5. ACKNOWLEDGEMENTS

This work performed under the auspices of the U.S. Department of Energy by LANL under contract DE-AC52-06NA25396 and by LLNL under Contract DE-AC5 2-07NA27344.

6. REFERENCES

[1] J. Lindl, Development of the indirect-drive approach to inertial confinement fusion and the target physics basis for ignition and gain, Physics of Plasmas **2** (1995) 3933.
[2] D. C. Wilson, e. al., and The Development and Advantages of Beryllium Capsules fo r the National Ignition Facility,, Phys. Plasmas (1998).
[3] S. W. Haan *et al.*, Design and simulations of indirect drive ignition targets for NIF, Nuclear Fusion **44** (2004) S171, Pii s0029-5515(04)88467-9.
[4] S. W. Haan *et al.*, NIF IGNITION CAMPAIGN TARGET PERFORMANCE AND REQUIREMENTS: STATUS MAY 2012, Fusion Science and Technology **63** (2013) 67.
[5] S. W. Haan *et al.*, Update 2015 on Target Fabrication Requirements for NIF Layered Implosions, with Emphasis on Capsule Support and Oxygen Modulations in GDP, Fusion Science and Technology **70** (2016) 121.
[6] R. B. Stephens, S. W. Haan, and D. C. Wilson, Characterization Specifications for Baseline Indirect Drive NIF Targets, Fusion Science and Technology **41** (2002) 226.
[7] J. A. Paisner, E. M. Campbell, and W. J. Hogan, The National Ignition Facility protect, Fusion Technology **26** (1994) 755.
[8] S. H. Glenzer *et al.*, Cryogenic thermonuclear fuel implosions on the National Ignition Facility, Physics of Plasmas **19** (2012) 15, 056318.
[9] S. H. Glenzer *et al.*, First implosion experiments with cryogenic thermonuclear fuel on the National Ignition Facility, Plasma Physics and Controlled Fusion **54** (2012) 13, 045013.
[10] S. W. Haan *et al.*, Point design targets, specifications, and requirements for the 2010 ignition campaign on the National Ignition Facility, Physics of Plasmas **18** (2011), 051001.
[11] T. Ma *et al.*, Onset of Hydrodynamic Mix in High-Velocity, Highly Compressed Inertial Confinement Fusion Implosions, Physical Review Letters **111** (2013) 5, 085004.
[12] S. P. Regan *et al.*, Hot-Spot Mix in Ignition-Scale Inertial Confinement Fusion Targets, Physical Review Letters **111** (2013) 5, 045001.
[13] S. W. Haan, WEAKLY NONLINEAR HYDRODYNAMIC INSTABILITIES IN INERTIAL FUSION, Physics of Fluids B-Plasma Physics **3** (1991) 2349.
[14] N. M. Hoffman, *Hydrodynamic instabilities in inertial confinement fusion* (Scottish Univ Summer School Physics Publications, Edinburgh, 1995), Vol. 45, Laser Plasma Interactions 5: Inertial Confinement Fusion.
[15] J. D. Kilkenny *et al.*, *EXPERIMENTAL-DETERMINATION OF THE HYDRODYNAMIC INSTABILITY GROWTH-RATES IN INDIRECT AND DIRECT-DRIVE ICF* 1993), Plasma Physics and Controlled Nuclear Fusion Research 1992, Vol 3.
[16] R. P. J. Town *et al.*, Dynamic symmetry of indirectly driven inertial confinement fusion capsules on the National Ignition Facility, Physics of Plasmas **21** (2014) 9, 056313.
[17] M. J. Edwards *et al.*, Progress towards ignition on the National Ignition Facility, Physics of Plasmas **20** (2013) 10, 070501.
[18] D. S. Clark *et al.*, Detailed implosion modeling of deuterium-tritium layered experiments on the National Ignition Facility, Physics of Plasmas **20** (2013) 14, 056318.
[19] O. A. Hurricane *et al.*, The high-foot implosion campaign on the National Ignition Facility, Physics of Plasmas **21** (2014) 056314, 056314.
[20] T. R. Dittrich *et al.*, Design of a High-Foot High-Adiabat ICF Capsule for the National Ignition Facility, Physical Review Letters **112** (2014) 055002, 055002.

[21] O. A. Hurricane *et al.*, Fuel gain exceeding unity in an inertially confined fusion implosion, Nature **506** (2014) 343.
[22] H. S. Park *et al.*, High-Adiabat High-Foot Inertial Confinement Fusion Implosion Experiments on the National Ignition Facility, Physical Review Letters **112** (2014) 055001, 055001.
[23] J. L. Peterson, P. Michel, C. A. Thomas, and R. P. J. Town, The impact of laser plasma interactions on three-dimensional drive symmetry in inertial confinement fusion implosions, Physics of Plasmas **21** (2014) 10, 072712.
[24] W. L. Kruer, S. C. Wilks, B. B. Afeyan, and R. K. Kirkwood, Energy transfer between crossing laser beams, Physics of Plasmas **3** (1996) 382.
[25] P. Michel *et al.*, Tuning the Implosion Symmetry of ICF Targets via Controlled Crossed-Beam Energy Transfer, Physical Review Letters **102** (2009), 025004.
[26] P. Michel *et al.*, Symmetry tuning via controlled crossed-beam energy transfer on the National Ignition Facility, Physics of Plasmas **17** (2010), 056305.
[27] J. D. Moody *et al.*, Progress in hohlraum physics for the National Ignition Facility, Physics of Plasmas **21** (2014), 056317.
[28] D. S. Clark *et al.*, Three-dimensional simulations of low foot and high foot implosion experiments on the National Ignition Facility, Physics of Plasmas **23** (2016) 056302, 056302.
[29] S. R. Nagel *et al.*, Effect of the mounting membrane on shape in inertial confinement fusion implosions, Physics of Plasmas **22** (2015) 022704, 022704.
[30] R. Tommasini *et al.*, Tent-induced perturbations on areal density of implosions at the National Ignition Facility, Physics of Plasmas **22** (2015) 056315, 056315.
[31] N. B. Meezan *et al.*, Indirect drive ignition at the National Ignition Facility, Plasma Physics and Controlled Fusion **59** (2017), 014021.
[32] L. F. B. Hopkins *et al.*, Near-vacuum hohlraums for driving fusion implosions with high density carbon ablators, Physics of Plasmas **22** (2015), 056318.
[33] L. F. B. Hopkins *et al.*, First High-Convergence Cryogenic Implosion in a Near-Vacuum Hohlraum, Physical Review Letters **114** (2015), 175001.
[34] N. B. Meezan *et al.*, Cryogenic tritium-hydrogen-deuterium and deuterium-tritium layer implosions with high density carbon ablators in near-vacuum hohlraums, Physics of Plasmas **22** (2015), 062703.
[35] S. Le Pape *et al.*, The near vacuum hohlraum campaign at the NIF: A new approach, Physics of Plasmas **23** (2016), 056311.
[36] S. Le Pape *et al.*, Fusion Energy Output Greater than the Kinetic Energy of an Imploding Shell at the National Ignition Facility, Physical Review Letters **120** (2018) 6, 245003.
[37] R. Betti *et al.*, Thermonuclear ignition in inertial confinement fusion and comparison with magnetic confinement, Physics of Plasmas **17** (2010), 058102.
[38] B. L. Cheng, T. J. T. Kwan, Y. M. Wang, and S. H. Batha, On thermonuclear ignition criterion at the National Ignition Facility, Physics of Plasmas **21** (2014) 6, 102707.
[39] O. S. Jones *et al.*, Progress towards a more predictive model for hohlraum radiation drive and symmetry, Physics of Plasmas **24** (2017), 056312.
[40] D. A. Callahan *et al.*, Exploring the limits of case-to-capsule ratio, pulse length, and picket energy for symmetric hohlraum drive on the National Ignition Facility Laser, Physics of Plasmas **25** (2018), 056305.
[41] G. N. Hall *et al.*, The relationship between gas fill density and hohlraum drive performance at the National Ignition Facility, Physics of Plasmas **24** (2017), 052706.
[42] A. L. Kritcher *et al.*, Metrics for long wavelength asymmetries in inertial confinement fusion implosions on the National Ignition Facility, Physics of Plasmas **21** (2014) 10, 042708.
[43] L. Divol *et al.*, Symmetry control of an indirectly driven high-density-carbon implosion at high convergence and high velocity, Physics of Plasmas **24** (2017), 056309.
[44] D. L. Bleuel and et al., Neutron activation diagnostics at the National Ignition Facility, Rev. Sci. Instrum. **83** (2012).
[45] V. Yu and et al., The National Ignition Facility neutron time-of-flight system and its initial performance, Rev. Sci. Instrum. **81** (2010).
[46] R. A. Lerche and et al., National Ignition Facil- ity neutron time-of-flight measurements, Rev. Sci. Instrum. (2010).
[47] M. G. Johnson *et al.*, Indications of flow near maximum compression in layered deuterium-tritium implosions at the National Ignition Facility, Physical Review E **94** (2016), 021202.

[48] F. E. Merrill *et al.*, The neutron imaging diagnostic at NIF (invited), Review of Scientific Instruments **83** (2012) 10D317.
[49] P. L. Volegov, C. R. Danly, D. Fittinghoff, V. Geppert-Kleinrath, G. Grim, F. E. Merrill, and C. H. Wilde, Three-dimensional reconstruction of neutron, gamma-ray, and x-ray sources using spherical harmonic decomposition, Journal of Applied Physics **122** (2017), 175901.
[50] R. Tommasini *et al.*, Development of Compton radiography of inertial confinement fusion implosions, Phys. Plasmas **18** (2011).
[51] O. Landen, 2018).
[52] S. Bhandarkar *et al.*, Fabrication of Low-Density Foam Liners in Hohlraums for NIF Targets, Fusion Science and Technology **73** (2018) 194.
[53] Y. Xu, T. Zhu, S. Li, and J. Yang, Beneficial effect of CH foam coating on x-ray emission from laser-irradiated high-Z material, Physics of Plasmas **18** (2011), 053301.
[54] P. Amendt, C. Cerjan, D. E. Hinkel, J. L. Milovich, H. S. Park, and H. F. Robey, Rugby-like hohlraum experimental designs for demonstrating x-ray drive enhancement, Physics of Plasmas **15** (2008), 012702.
[55] M. Vandenboomgaerde, J. Bastian, A. Casner, D. Galmiche, J. P. Jadaud, S. Laffite, S. Liberatore, G. Malinie, and F. Philippe, Prolate-spheroid ("Rugby-Shaped") hohlraum for inertial confinement fusion, Physical Review Letters **99** (2007), 065004.
[56] P. Amendt *et al.*, Low-adiabat rugby hohlraum experiments on the National Ignition Facility: Comparison with high-flux modeling and the potential for gas-wall interpenetration, Physics of Plasmas **21** (2014), 112703.
[57] P. E. Masson-Laborde *et al.*, Laser plasma interaction on rugby hohlraum on the Omega Laser Facility: Comparisons between cylinder, rugby, and elliptical hohlraums, Physics of Plasmas **23** (2016), 022703.
[58] H. F. Robey, L. B. Hopkins, J. L. Milovich, and N. B. Meezan, The I-Raum: A new shaped hohlraum for improved inner beam propagation in indirectly-driven ICF implosions on the National Ignition Facility, Physics of Plasmas **25** (2018) 10, 012711.
[59] D. A. Martinez *et al.*, Hydro-instability growth of perturbation seeds from alternate capsule-support strategies in indirect-drive implosions on National Ignition Facility, Physics of Plasmas **24** (2017), 102707.
[60] C. R. Weber *et al.*, Improving ICF implosion performance with alternative capsule supports, Physics of Plasmas **24** (2017), 056302.
[61] V. A. Smalyuk *et al.*, First Measurements of Hydrodynamic Instability Growth in Indirectly Driven Implosions at Ignition-Relevant Conditions on the National Ignition Facility, Physical Review Letters **112** (2014), 185003.
[62] B. M. Haines *et al.*, The effects of convergence ratio on the implosion behavior of DT layered inertial confinement fusion capsules, Physics of Plasmas **24** (2017) 12, 072709.
[63] L. A. Pickworth *et al.*, Visualizing deceleration-phase instabilities in inertial confinement fusion implosions using an "enhanced self-emission" technique at the National Ignition Facility, Physics of Plasmas **25** (2018) 8, 054502.
[64] V. A. Smalyuk *et al.*, Review of hydro-instability experiments with alternate capsule supports in indirect-drive implosions on the National Ignition Facility, Physics of Plasmas **25** (2018), 072705.
[65] B. A. Hammel *et al.*, A "polar contact" tent for reduced perturbation and improved performance of NIF ignition capsules, Physics of Plasmas **25** (2018), 082714.
[66] L. B. Hopkins, EPS paper (2018).
[67] J. Biener *et al.*, Diamond spheres for inertial confinement fusion, Nuclear Fusion **49** (2009) 5, 112001.
[68] A. J. MacKinnon *et al.*, High-density carbon ablator experiments on the National Ignition Facility, Physics of Plasmas **21** (2014) 11, 056318.
[69] H. Takabe, K. Mima, L. Montierth, and R. L. Morse, Self-consistent growth rate of the Rayleigh-Taylor instability in an ablatively accelerating plasma, Phys. Fluids **28** (1985).
[70] L. B. Hopkins *et al.*, Increasing stagnation pressure and thermonuclear performance of inertial confinement fusion capsules by the introduction of a high-Z dopant, Physics of Plasmas **25** (2018) 080706.
[71] L. A. Pickworth *et al.*, in *9th International Conference on Inertial Fusion Sciences and Applications*, edited by E. Storm2016).
[72] L. A. Pickworth *et al.*, Visualizing deceleration-phase instabilities in inertial confinement fusion implosions using an "enhanced self-emission" technique at the National Ignition Facility, Physics of Plasmas **25** (2018), 054502.
[73] G. N. Hall and e. al., in preparation for Review of Scientific Instruments (2018).
[74] S. Palaniyappan and e. al., in preparation for Phys. Plasmas (2018).

[75] L. B. Hopkins *et al.*, Increasing stagnation pressure and thermonuclear performance of inertial confinement fusion capsules by the introduction of a high-Z dopant, Physics of Plasmas **25** (2018), 080706.
[76] R. Nora *et al.*, Theory of hydro-equivalent ignition for inertial fusion and its applications to OMEGA and the National Ignition Facility, Physics of Plasmas **21** (2014) 14, 056316.
[77] P.-T. Bremer, D. Maljovec, A. Saha, B. Wang, J. Gaffney, B. K. Spears, and V. Pascucci, $$\mathrm{ND}^2\mathrm{AV}$$ND2AV: N-dimensional data analysis and visualization analysis for the National Ignition Campaign, Computing and Visualization in Science **17** (2015) 1.
[78] S. H. Langer, B. Spears, J. L. Peterson, J. E. Field, R. Nora, S. Brandon, and Ieee, *A HYDRA UQ Workflow for NIF Ignition Experiments* 2016), Proceedings of Isav 2016: 2nd Workshop on in Situ Infrastructures for Enabling Extreme-Scale Analysis and Visualization.
[79] R. Nora, J. L. Peterson, B. K. Spears, J. E. Field, and S. Brandon, Ensemble simulations of inertial confinement fusion implosions, Stat. Anal. Data Min. **10** (2017) 230.
[80] K. D. Humbird, J. L. Peterson, and R. G. McClarren, Deep Jointly-Informed Neural Networks arXiv, arXiv (USA) (2017) 7 pp.
[81] C. J. Stolz *et al.*, in *SPIE Optical Systems Design* (SPIE, 2018), p. 12.
[82] L. J. Suter *et al.*, Prospects for high-gain, high yield National Ignition Facility targets driven by 2 omega (green) light, Physics of Plasmas **11** (2004) 2738.
[83] K. R. Manes *et al.*, Damage Mechanisms Avoided or Managed for NIF Large Optics, Fusion Science and Technology **69** (2016) 146.
[84] M. L. Spaeth *et al.*, Optics Recycle Loop Strategy for NIF Operations Above UV Laser-Induced Damage Threshold, Fusion Science and Technology **69** (2016) 265.